

# Optimization of Wireless Sensor Network and UAV Data Acquisition

Dac-Tu Ho<sup>1,2</sup> · Esten Ingar Grøtli<sup>1,3</sup> · P. B. Sujit<sup>4</sup> · Tor Arne Johansen<sup>1,5</sup> · João Borges Sousa<sup>4</sup>

Received: date / Accepted: date

**Abstract** This paper deals with selection of sensor network communication topology and the use of Unmanned Aerial Vehicles (UAVs) for data gathering. The topology consists of a set of cluster heads that communicate with the UAV. In conventional wireless sensor networks Low Energy Adaptive Clustering Hierarchy (LEACH) is commonly used to select cluster heads in order to conserve energy. Energy conservation is far more challenging for large scale deployments. Particle Swarm Optimization (PSO) is proposed as an optimization method to find the optimal topology in order to reduce the energy consumption, bit error rate (BER), and UAV travel time. PSO is compared to LEACH using a simulation case and the results show that PSO outperforms LEACH in terms of energy consumption and BER, while the UAV travel time is similar. The numerical results further illustrate that the performance gap between them increases with the number of cluster head nodes. Because of reduced energy consumption, network life time can be significantly extended while increasing the amount of data received from the entire network. By considering the wind effect into the PSO scheme, it is shown that this has an impact on

the traveling time for the UAV but BER and energy consumption are not significantly increased.

**Keywords** Unmanned Aerial Vehicle (UAV) · Data Mule · Particle Swarm Optimization (PSO) · Waypoint · Wireless Sensor Network (WSN)

## 1 Introduction

Unmanned Aerial Systems (UASs) technology has spread widely and become popular in various military and civilian fields. Some of the popular applications are radar localization [1], wildfire management, observation support [2], agricultural monitoring, border surveillance and monitoring, environmental and meteorological monitoring, and aerial photography [3], as well as for search and rescue missions [4]. The most noticeable benefits compared with conventional manned vehicles are low cost, improved safety for humans, and easy deployment. There are also many applications in Wireless Sensor Networks (WSNs) that employ Unmanned Aerial Vehicles (UAVs) to extend the range of communication [5], maximize the data communication capability of the network by using vehicles as relay nodes [6], collect data from a wide area network in remote or harsh environment [7], or aid node's localization in mobile network [8]. The key strategic research activities of the authors of this paper are within oil spill response, ice monitoring, ship traffic surveillance, and marine monitoring and operations. Many of the geographical areas of interest are harsh, remote and also isolated due to lack of communication infrastructure.

Building permanent communication infrastructure may be considered too expensive and difficult to maintain. It is easier and cheaper to set up a network of nodes on the ground or on the sea surface, and use

---

Corresponding author: D. T. Ho  
Tel.: +47 93 00 61 85.

E-mail: tudac.ho at marintek.sintef.no ·

<sup>1</sup>Department of Engineering Cybernetics, Norwegian University of Science and Technology.

O. S. Bragstads plass 2D, 7491 Trondheim, Norway ·

<sup>2</sup>Department of Maritime Transport Systems, MARINTEK. Otto Nielsens veg 10, 7491 Trondheim, Norway ·

<sup>3</sup>SINTEF ICT Applied Cybernetics.

PO 4760 Sluppen, 7465 Trondheim, Norway ·

<sup>4</sup> Department of Electrical and Computer Engineering, Faculdade de Engenharia da Universidade do Porto, Portugal ·

<sup>5</sup> Center for Autonomous Marine Operations and Systems

UAVs to gather data from these nodes. Extensive studies on how to gather data from wireless sensor nodes are surveyed in [9]. In these networks, sensor nodes are condensed and usually connected to each other in clusters. These nodes therefore communicate with the base station (sink) via their cluster head (CH) node. Hence, it requires multi-hop data communication between the nodes, which may consume a large amount of energy due to heavy communication and overhead messages exchanged among them for instance for clustering and receiving as well as forwarding of data to the sink by the cluster heads. This problem could be reduced by mobile sinks [10]. Optimal strategies for the mobile sink movements depends on the size of the WSN and how frequently it receives status information from the other nodes in the network [11]. However, the mobile sink solution still requires significant energy consumption when the nodes send information to the sink during its movement. The energy burden on each node could be further reduced when UAVs play the role of a sink node, as it flies over the network and receives data from as many nodes as possible [12]. UAVs are typically in line-of-sight (LOS) so they have better channel compared to surface vehicles. As with all moving sinks, it can be controlled to improve performance of the whole network. In [13], a new communication protocol (MAC) is introduced for the UAV and the nodes to minimize their energy usage and maximize network life time. Similarly, [14] proposed a heuristic algorithm for the UAV to search and retrieve data from the nodes by adaptively adjusting the UAV's path with the assumption that the UAV can only visit the CH node of each cluster. In many cases, multiple UAVs are used and coordination is necessary to find the optimal flight path. Path planning for the UAVs under dominant constraints such as inter-vehicle communication, collision avoidance and anti-grounding, is challenging and have been studied using methods suitable for preplanning [15], [16] and online methods suitable for re-planning [17]. In the presence of multiple agents, the CHs can be partitioned into subsets and allocated to each agent such that the time taken by these agents in visiting all the allocated CHs can be minimized. In [18] and [19], efficient centralized and distributed techniques to form clusters of CHs and allocation of these clusters to multi-robot teams to minimize the global cost was addressed. Our paper has a different approach from existing proposed methodologies in data gathering. We use a UAV as a data mule in order to gather data from a wide area wireless sensor networks and it then can transmit this data to a base station at its convenience. Our algorithm aims to find the optimal WSN communication topology and UAV path while taking into account en-

ergy consumption, bit error rate of all network nodes and the UAV's flight time.

## 2 Related Work and Contributions

The problem of optimal waypoint planning for UAVs under different constraints has been a study for a decade [20]. Depending on the applications, the objective functions and optimization methods are different. In this paper, the objective is to minimize the total energy consumption of the nodes; maximize the quality of data communication via wireless channel between any node and its CH, and between the CHs and the UAV; and minimize the flight time for the UAV. The target is to provide a list of nodes, which are then to be visited by the UAV. The optimization runs before every UAV flight mission, and its solution provides a path for the UAV to follow in order to complete one round of data collection.

Regarding the communication quality for the WSN and a UAV, [21] showed that lower Bit Error Rate (BER) is obtained if the UAV communicates with fewer sensor nodes at a time. However, the flight time will be significantly increased if the UAV needs to fly over all the nodes in the network. This issue was relaxed in [14] where the nodes were grouped in clusters and only the CHs were visited by the UAV. The clustering technique in [14] was only depending on the communication ability or distance, and this may be inefficient leading to poor communication quality or low energy efficiency. The optimal number of CHs for minimizing the time to visit all the nodes here is similar to the studies in Covering Salespersons Problem (CSP). In CSP, the objective is to minimize the total traveling time or distance for the salesperson to visit at least one element in disjoint subsets [22]. If the cluster is larger then the energy consumption for data forwarding is very high which is inefficient. [14], [21] and [22] have shown that there is a relation between the communication quality (BER) and the traveling distance or time of the UAV in our network model. This can also be seen in Section 4 of this paper. The energy consumption in traditional sensor networks is a challenging issue and it relates to cross-layer design such as network topology, clustering algorithms, transmissions method, and MAC protocol. In our previous papers, an energy-efficient MAC protocol [14] and a network coding method [7] have been proposed for wide area sensor networks.

LEACH is a clustering algorithm aimed at conserving energy of WSNs. It is a distributed scheme without any central node. In LEACH, each node can independently decide whether to become a CH or not depending on some probabilistic function [23]. The number of

CHs may vary, and the independent decision of whether or not to become a CH may lead to accelerated energy drainage for some of the nodes in the network. LEACH-C is a centralized scheme, which can improve the existing issues of LEACH. In LEACH-C, the information about location and residual energy of all nodes are sent to the base station (sink) at the beginning of each UAV flight. The base station will then calculate the average energy level in the network, and only nodes with energy above this level are considered for CH nodes. The base station will randomly select some candidates among these nodes and calculate the respective objective function. This procedure is repeated for a number of iterations, and the objective function value is compared in order to find the most suitable set of CHs. In the WSN literature it is common that the objective function is based on the average distances between CHs and their member nodes. The selected CH nodes are broadcast by the UAV to all the nodes in the network. Each node in the network finds the closest CH node to initiate its data transmission.

In conventional WSNs, Low Energy Adaptive Clustering Hierarchy-Centralized (LEACH-C) is popular in various applications because of its efficiency and low computational burden on nodes [24], [23]. However, in large area sensor networks, the energy conservation is far more challenging than for smaller WSNs and a better optimization method is necessary. Taking the advantage of energy and computational capabilities of the UAS (Unmanned Aerial System) compared to a normal sensor node, a population based iterative optimization technique, Particle Swarm Optimization (PSO), is used to determine the set of CHs. The results are compared with LEACH-C under the same conditions. In Section 3 we explain in detail how the PSO scheme is constituted and modified in order to be applied in our network optimization problem.

**A standing assumption in this paper is that the mission is carried out in an outdoor environment and that the nodes are deployed over a relatively flat terrain, therefore radio propagation path loss model used in this paper is a circular model with a radius. For the cases with deep fading and heavy reflections from the objects or obstructions such as the complex models for indoor or outdoor urban environments, these models developed in [25] and [?] would be the ideal ones to be implemented. We would still like to emphasize that the same framework presented in this paper could be used with more complex path loss models. The assumption of relatively flat terrain could for instance be relaxed by using the 'Longley-Rice Irregular Terrain' model or the 'Irregular Terrain With Obstructions' models, both of**

**which are implemented in the simulation tool SPLAT!, [26].**

The main contributions of this paper are (i) formulation of a multi-objective optimization problem for cluster head selection in a sensor network for UAV data acquisition (ii) considering realistic models and constraints on bit error rate, energy of the nodes, flight time of the UAV, and wind effects on the UAV (iii) comparing with existing LEACH-C algorithm in optimization for WSN data collection.

### 3 Particle Swarm Optimization Algorithm

Many applications in WSN use PSO as an efficient algorithm for making clusters of nodes [27], [28]. The idea behind PSO is to simulate the social behavior of bird flocks and fish schools [29]. The PSO algorithm is a computational method that iteratively tries to improve a swarm of candidate solutions or particles, based on a few basic rules. For each particle  $i \in \{1, \dots, S\}$ , where  $S$  is the number of particles, the particle position,  $x_i \in \mathbb{R}^n$ , and the particle velocity,  $v_i \in \mathbb{R}^n$ , is updated according to

$$x_i \leftarrow x_i + v_i, \quad (1)$$

and

$$v_i \leftarrow \omega v_i + c_p r_p (p_i - x_i) + c_g r_g (g - x_i), \quad (2)$$

respectively. Here,  $r_p, r_g \sim U(0, 1)$ , *i.e.* they are drawn from a uniform distribution between 0 and 1,  $p_i$  is the best known position of particle  $i$ ,  $g$  is the best known position of the swarm, and  $\omega$  (inertia weight),  $c_p$  and  $c_g$  (acceleration constants) are tuning parameters. The fitness of a solution is calculated based on the value of a function  $f : \mathbb{R}^n \rightarrow \mathbb{R}$ , which is to be minimized. A particle's best known position is updated, that is,  $p_i \leftarrow x_i$ , if  $f(x_i) < f(p_i)$ . The swarm's best known position is updated, that is,  $g \leftarrow p_i$ , if  $f(p_i) < f(g)$ . The inertial weight ( $\omega$ ) balances between global and local exploration. Typically, the value of  $\omega$  is high at the beginning of the simulation with enables the PSO to explore the search space. As the number of iterations increase in the simulations, the  $\omega$  reduces thus exploring the local search space[30]. The constants ( $c_p$  and  $c_g$ ) help in achieving convergence of the solution. The random parameters ( $r_1$  and  $r_2$ ) maintain the diversity of the swarm population which is essential in seeking a good solution.

The initial positions of the particles are uniformly distributed in the search space, *i.e.*  $x_{id} \sim U(\underline{b}_d, \bar{b}_d)$ , where  $d$  is the dimension of the search space and  $\underline{b}_d, \bar{b}_d$

are the lower and upper bounds, respectively. The particles initial velocities in any direction  $d$  of the search space are  $v_{id} \sim U(-|\bar{b}_d - \underline{b}_d|, |\bar{b}_d - \underline{b}_d|)$ . The algorithm is terminated after a user specified number of iterations, or some other criterion depending on the fitness function.

One of the advantages of PSO is that it does not rely explicitly on the gradient information of the optimization problem, unlike many of the classical methods. The main disadvantage is that it does not guarantee that an optimal solution is found. Some attempts at analyzing the convergence properties of PSO exists in the literature, for instance [31], [32], but oversimplifying assumptions [33].

Each particle  $x_i$  is a candidate solution containing the position vector of a CH. Let  $N^{\text{CH}}$  be the number of CHs, and let  $N$  be the number of sensors in our sensor network. We are furthermore concerned with a two dimensional problem, and the position of each sensor is known. Since  $x_i$  contains a candidate solution for the positions of all the  $N^{\text{CH}}$  CHs, the length of the vector  $x_i$  is  $n = 2N^{\text{CH}}$ . To force the CH positions to be chosen from the sensor positions, we introduce the function  $h : \mathbb{R}^{2N^{\text{CH}}} \rightarrow \mathbb{R}^{2N^{\text{CH}}}$ , which takes the particle position vector  $x_i$ , and return the position vector of the  $N^{\text{CH}}$  sensors closest to  $x_i$ . For instance, if  $x_i = (x_{i1}^\top, x_{i2}^\top, \dots, x_{iN^{\text{CH}}}^\top)^\top$ , then  $h(x_i) = (\tilde{x}_1^{\star\top}, \tilde{x}_2^{\star\top}, \dots, \tilde{x}_{N^{\text{CH}}}^{\star\top})^\top$ , where  $\tilde{x}_1^*, \tilde{x}_2^*, \dots, \tilde{x}_{N^{\text{CH}}}^*$  are the optimal CH locations achieved by solving an assignment problem. Here, the assignment problem is typically unbalanced since the number of sensor locations is greater than the number of CHs, but can be balanced by introducing additional dummy variables. The solution can be found efficiently by employing the Hungarian algorithm, [34], or by numerical optimization of the linear programming problem formally stated as:

$$\min \sum_{j=1}^N \sum_{k=1}^N C_{j,k} z_{j,k} \quad (3)$$

subject to the constraints

$$\sum_{k=1}^N z_{j,k} = 1, \quad \text{for } j \in \{1, 2, \dots, N\}, \quad (4)$$

$$\sum_{j=1}^N z_{j,k} = 1, \quad \text{for } k \in \{1, 2, \dots, N\}, \quad (5)$$

$$z_{j,k} \geq 0, \quad \text{for } j, k \in \{1, 2, \dots, N\} \quad (6)$$

and where for any  $j, k \in \{1, 2, \dots, N\}$

$$C_{j,k} = \begin{cases} \|\tilde{x}_k - x_{ij}\| & \text{if } j \leq N^{\text{CH}} \\ 0 & \text{if } j > N^{\text{CH}} \end{cases} \quad (7)$$

Here,  $\tilde{x}_k$  is the location of sensor  $k$ ,  $z_{j,k}$  is the optimization variable assigning the  $j$ -th position coordinate of the candidate solution  $x_i$  to sensor  $k$ , and  $C_{j,k}$  is the corresponding costs.

The optimal CHs are chosen based on a fitness function,

$$f = \alpha_1 f_1 + \alpha_2 f_2 + \alpha_3 f_3 \quad (8)$$

where  $\alpha_1, \alpha_2, \alpha_3 > 0$  are scalar weighting constants that reflect the priorities or expectations of optimizing the sub functions  $f_1, f_2$ , or  $f_3$ , respectively.  $f_1$  is the energy consumption of all nodes in the network caused by information exchange and data transmission with the UAV;  $f_2$  is the transmission BER of data communication between the UAV and the nodes; and  $f_3$  is the total travel time for the UAV to fly from the original point, cover the entire set of CHs, and back to the original point. Depending on the objective of the optimization algorithm, the actual values of  $\alpha_1, \alpha_2, \alpha_3$  would be changed accordingly. The way of choosing these weighting constants as well as their variations in different cases of dominant sub functions are deeply discussed in Section 4.3. These variations would lead to changes in the result of the optimization and therefore system (network) performance as well, which will be illustrated in details in the simulation results, Section 4. Before that, each sub function will be thoroughly explained in the following sections.

The process of determining the CHs using PSO is summarized in Algorithm 1. The main inputs of this scheme are the known positions of the sensor nodes, the upper and lower bounds for the search space optimization, the number of iterations, the number of sensor nodes, and the number of waypoints (CH nodes) for the UAV.

### 3.1 Network energy consumption

The total energy consumption for a non-cluster head node  $j$  transmitting information to CH  $i$  is calculated as the sum of energy for transmitting a data packet, and transmitting and receiving a control packet which is

$$E_j = lE_{ji} + l_{\text{ctr}} \frac{Pt_0}{R_0} + E_{\text{RX}} l_{\text{ctr}}, \quad (9)$$

where,  $l$  is the data packet length in bits,  $l_{\text{ctr}}$  is the number of bits in a control packet,  $E_{ji}$  is the energy to transmit one bit from node  $j$  to the CH of the  $i$ -th cluster,  $Pt_0$  is standard TX power,  $E_{\text{RX}}$  is the energy consumed to receive one bit, and  $R_0$  is the bit rate

**Algorithm 1** - PSO

---

**Require:**  $\bar{b}, \omega, c_p, c_g$   
**for**  $i \in \{1, \dots, S\}$  **do** ▷ Start initializing  
     **for**  $d \in \{1, \dots, n\}$  **do**  
          $x_{id} \sim U(\underline{b}_d, \bar{b}_d)$   
          $v_{id} \sim U(-|\bar{b}_d - \underline{b}_d|, |\bar{b}_d - \underline{b}_d|)$   
     **end for**  
      $p_i \leftarrow x_i$   
     **if**  $i = 1$  **then**  
          $g \leftarrow x_1$   
     **else if**  $f(h(p_i)) \leq f(h(g))$  **then**  
          $g \leftarrow p_i$   
     **end if**  
**end for** ▷ End initializing  
 $k \leftarrow 1$   
**while**  $k \leq N_{\text{Iterations}}$  **do**  
     **for**  $i \in \{1, \dots, S\}$  **do**  
          $r_p, r_g \sim U(0, 1)$   
         **for**  $d \in \{1, \dots, n\}$  **do**  
              $v_{id} \leftarrow \omega v_{id} + c_p r_p (p_{id} - x_{id}) + c_g r_g (g - x_{id})$   
         **end for**  
          $x_i \leftarrow x_i + v_i$   
         **if**  $f(h(x_i)) \leq f(h(p_i))$  **then**  
              $p_i \leftarrow x_i$   
             **if**  $f(h(p_i)) \leq f(h(g))$  **then**  
                  $g \leftarrow p_i$   
             **end if**  
         **end if**  
     **end for**  
      $k \leftarrow k + 1$   
**end while**  
**return**  $g$

---

used in broadcasting messages. The expression for  $E_{ji}$  is given by

$$E_{ji} = \frac{Pt_{ji}}{R_{ji}} = \begin{cases} \frac{Pt_0}{R_{ji}} & \text{if } Pr_{ji} > Pr_{\min} \\ \frac{Pt_{\min}}{R_b} & \text{if } Pr_{ji} \leq Pr_{\min} \end{cases}, \quad (10)$$

where, the transmit power is adjusted based on link budget estimation between node  $j$  and its CH  $i$ .  $Pt_{ji}$  and  $R_{ji}$  are the transmit power and respective bit rate of the communication channel between node  $j$  and its CH node  $i$ . In the first case,  $Pr_{ji} = Pt_0 + G_{ij} - PL_{ji} > Pr_{\min}$ , where  $PL_{ji}$  is the path loss between node  $j$  and CH  $i$ , and CH  $i$  can receive data from node  $j$  with the standard transmission power,  $Pt_0$ . In the second case,  $Pr_{ji} = Pt_0 + G_{ij} - PL_{ji} \leq Pr_{\min}$ , and transmission power is controlled to increase node  $j$ 's transmit power to  $Pt_{\min} = PL_{ji} + Pr_{\min} - G_{ij}$  such that CH  $i$  can receive data at a basic rate,  $R_b$ , according to receiving strength of  $Pr_{\min}$  and  $G_{ij}$  is the total gain of antennas on node  $j$  and CH  $i$ . **Under the assumption that the sensor nodes are distributed in an outdoor environment on a relatively flat surface or terrain and the distances between the nodes are large compared to the heights of their antennas**, the actual propagation path loss  $PL_{ji}$  between node  $j$  and CH  $i$  can be extracted from the

standard two-ray path loss model [35, Page 35],

$$PL_{ji} = 40 \log d_{ji} - 20 \log h_i - 20 \log h_j, \quad (11)$$

where  $h_j$  and  $h_i$  are the heights above ground or surface of the node's antennas, and  $d_{ji}$  is the distance between them. In wide area sensor network, the nodes are not close to each other so it is reasonable to assume that CH  $i$  will receive and forward the data of its member nodes to the UAV. Therefore, in the  $i$ -th cluster, the total energy consumption by the CH to receive and then forward its member node as well as transmitting its own data is

$$E_i = \left[ l(E_{\text{RX}} + E_{\text{DA}}) + lE_{iu} + E_{\text{RX}}l_{\text{ctr}} + l_{\text{ctr}} \frac{Pt_0}{R_0} \right] (N_i - 1) + lE_{\text{TX}} + lE_{\text{DA}} + l_{\text{ctr}}E_{\text{RX}} + l_{\text{ctr}} \frac{Pt_0}{R_0}, \quad (12)$$

where  $E_{\text{TX}}$ ,  $E_{\text{RX}}$  is the energy to transmit or receive one bit;  $E_{\text{DA}}$  is energy for data aggregation per bit, which is only applied to the CH nodes;  $E_{iu}$  is the energy consumption for sending one bit from CH  $i$  to the UAV;  $N_i$  is the number of member nodes in the  $i$ -th cluster. The first portion of this formula describes the energy for exchanging control packets, receiving data from member nodes, and transmitting their data to the UAV; the second part is the energy for sensing and transmitting this data of CH node  $i$  to the UAV. Other parameters are similar as in (9). Normally  $E_{\text{RX}}$  and  $E_{\text{TX}}$  are the same, so (12) could be written in a more compact form,

$$E_i = lN_i(E_{\text{RX}} + E_{\text{DA}}) + l_{\text{ctr}}N_i \frac{Pt_0}{R_0} + l_{\text{ctr}}N_iE_{\text{RX}} + l(N_i - 1)E_{iu}, \quad (13)$$

where  $N_i$  is the number of sensor nodes in cluster  $i$  including CH  $i$ ,  $E_{iu}$  is the energy per bit to transmit from CH  $i$  to the UAV (denoted with the subscript  $u$ ). The expression for  $E_{iu}$  is calculated similar as in (10),

$$E_{iu} = \frac{Pt_{iu}}{R_{iu}} = \begin{cases} \frac{Pt_0}{R_{iu}} & \text{if } Pr_{iu} > Pr_{\min} \\ \frac{Pt_{\min}}{R_b} & \text{if } Pr_{iu} \leq Pr_{\min} \end{cases}, \quad (14)$$

where  $Pt_{iu}$  is the necessary transmission power at node  $i$  when communicating with the UAV. In the first case the standard value  $Pt_0$  is large enough to maintain communication without power control, that is,  $Pr_{iu} = Pt_0 + G_{ij} - PL_{iu} > Pr_{\min}$ , where  $PL_{iu}$  is the path loss between CH  $i$  and the UAV. **Under the assumption that the UAV is flying over the nodes on a flat terrain without significant obstructions, the propagation path between the UAV and the nodes would usually be line of**

sight (LOS). In addition, the altitude of the UAV would always be significantly high compared to the nodes, so it is reasonable to apply free space path loss for  $PL_{iu}$ . Converting from a standard formula in [35, Page 32], we have that

$$PL_{iu} = -147.55 + 20 \log F + 20 \log d_{iu}, \quad (15)$$

where  $F$  is radio frequency in Hertz,  $d_{iu}$  is the distance between CH  $i$  and the UAV in meter. In the second case of (14),  $Pr_{iu} = Pt_0 + G_{iu} - PL_{iu} \leq Pr_{\min}$ , and power control is used such  $Pt_{\min} = PL_{iu} + Pr_{\min} - G_{iu}$  where  $G_{iu}$  is the total gain of the antennas at CH  $i$  and the UAV. Similar as to the case between two sensor nodes,  $Pt_{\min}$  is also calculated for this case which is between CH  $i$  and the UAV.

With the ability of calculating path loss function between two nodes or between a node and the UAV, it would be possible to estimate the energy consumption by each node in any of those cases. Therefore,  $f_1$ , the total energy for data communication between all of the member nodes and its CH node  $i$  as well as the energy used for forwarding all of the member node's data in addition with CH node's data to the UAV (by the CH  $i$ ), is described as in following equation:

$$f_1 = \sum_{i=1}^{N^{\text{CH}}} \sum_{j=1}^{N_i-1} E_{ji} + \sum_{i=1}^{N^{\text{CH}}} E_{iu}. \quad (16)$$

where the first sum is the total energy used for communication between the node  $j$  and CH node  $i$ , and the second part is the total energy used by all of the CH nodes for data communication with the UAV. The expressions for  $E_{iu}$  and  $E_{ji}$  are given in (10) and (14).

The total energy consumption depends on the deployed environment. In a different environment the propagation path loss model would have to be changed accordingly. In this paper we have assumed that mission is in an outdoor environment and that the nodes are deployed over a relatively flat terrain. This assumption could be relaxed by for instance using the 'Longley-Rice Irregular Terrain' model or the 'Irregular Terrain With Obstructions' models, both of which are implemented in the simulation tool SPLAT!, [26].

### 3.2 Bit error rate

The Bit Error Rate (BER) usually depends on data modulation scheme and communication channel between transmitter and receiver. In this sensor network model, we are most concerned about saving the nodes energy consumed by data communication. Therefore, M-QAM modulation is used for all the nodes. Following [35, Page

190], the average symbol error rate of this scheme is estimated by

$$\begin{aligned} \bar{P}_s = & \frac{4}{\pi} \left(1 - \frac{1}{\sqrt{Q}}\right) \int_0^{\pi/2} M_{\gamma_s}(\omega, \phi) d\phi \\ & - \frac{4}{\pi} \left(1 - \frac{1}{\sqrt{Q}}\right)^2 \int_0^{\pi/4} M_{\gamma_s}(\omega, \phi) d\phi, \end{aligned} \quad (17)$$

where  $Q$  is the modulation rate, and  $\omega = 1.5/(Q - 1)$ .  $M_{\gamma_s}(\omega, \phi)$  is a Moment Generating Function (MGF) which is used in performing analysis of modulation in fading with and without diversity, and  $\phi$  is the angle variable of the integrals.

If the radio channel is between any two nodes on the ground, then the reflection portion of radio paths on the ground is significant. For instance, the symbol error rate of the channel between a node  $j$  and its CH  $i$ , can be calculated using (17) with the Rayleigh multipath fading distribution [35, Page 189],

$$M_{\gamma_s,ji}(\omega, \phi) = \left(1 + \frac{\omega \bar{\gamma}_s}{\sin^2 \phi}\right)^{-1}. \quad (18)$$

Here,  $\bar{\gamma}_s$  denotes the average Signal to Interference plus Noise Ratio (SINR) at a fixed path loss over the channel. Basically, SINR is equal to  $S/(I + N_0)$ , where  $S$  is the expected signal strength at the receiver,  $I$  is interference from all the sources located around the receiver node, and  $N_0$  is the standard noise in the channel. For the communication between CH  $i$ , and the UAV  $u$  flying over it, the Line-of-Sight (LOS) signal strength is usually the dominant portion compared to the portion from other reflected signals, so (17) can be calculated with Rician multipath fading distribution [35, Page 189],

$$\begin{aligned} M_{\gamma_s,iu}(\omega, \phi) = & \frac{(1 + K) \sin^2 \phi}{(1 + K) \sin^2 \phi + \omega \bar{\gamma}_{s,iu}} \\ & \times \exp\left(\frac{K \omega \bar{\gamma}_{s,iu}}{(1 + K) \sin^2 \phi + \omega \bar{\gamma}_{s,iu}}\right). \end{aligned} \quad (19)$$

Here,  $K$  is the Rice factor and denotes the dominance of the LOS path over the reflection paths portion. From our prior research on air to ground communication system, the value of  $K$  could be varied according to the incident angle constituted by the arriving signal and the receiving node [36]. With the assumption that the UAV and the node are setup with small array antennas, so their relative distance and position would not affect the actual value of  $K$ . In the case where the antenna array is not existing on any of the node or the UAV, this effect must be taken into account.

In order to evaluate the BER, the symbol-error probability  $\bar{P}_s$  is converted into average bit-error probability

$P_b$  as follows

$$P_b = \frac{\bar{P}_s}{\log_2 Q}. \quad (20)$$

Then the general BER of the system which describes the sub function  $f_2$  introduced in (8), is calculated as the fraction between the total number of error bits (for both transmissions in the two cases: node to node and the CH node to the UAV) and the total bits transmitted by all of the nodes, as follow

$$f_2 = \frac{\sum_{i=1}^{N^{\text{CH}}} \sum_{j=1}^{N_i-1} P_{b,ji}l + \sum_{i=1}^{N^{\text{CH}}} P_{b,iu}l(N_i - 1)}{(2N - N^{\text{CH}})}, \quad (21)$$

where  $P_{b,ji}$  and  $P_{b,iu}$  are the probabilities of erroneous bits of the communication channels between node  $j$  and its CH  $i$ , and between CH  $i$  and the UAV, respectively.

### 3.3 UAV-path and travel time

Another sub fitness function  $f_3$  introduced in (8) is for the total travel time for the UAV which means the time it takes from its original position to visit all the CHs, and then return to the starting point. In the case of no wind effect, the UAV ground speed could be constant, and therefore the time spent is proportional to the total distance. [37] used the approximation algorithm to the Dubins' traveling salesperson problem of [38], in order to estimate the flying distance of the UAV. The wind is however a common effect that should be added into this network model. The effect is dependent on the wind speed and wind direction in the area. In order to estimate the total flight time of the UAV, the UAV kinematics can be modeled as the dependence on the current location, its own speed and heading angle, as well as the wind speed and its heading, as follow

$$\begin{aligned} \dot{x} &= v_a \cos \psi + v_w \cos \psi_w = v_g \cos \chi, \\ \dot{y} &= v_a \sin \psi + v_w \sin \psi_w = v_g \sin \chi, \\ \dot{\psi} &= k(\chi_d - \chi), \end{aligned} \quad (22)$$

where  $(x, y)^\top$  is the position of the UAV,  $\chi = \text{atan2}(\dot{y}, \dot{x})$ ,  $v_a$  is the UAV air speed,  $\psi$  is the heading angle,  $v_w$  is the wind speed,  $\psi_w$  is the wind direction,  $\chi_d$  is the desired direction towards the goal,  $\chi$  is the course angle,  $\dot{\chi}$  is the course angle rate, and the ground speed of the UAV is  $v_g = \sqrt{\dot{x}^2 + \dot{y}^2}$ , and  $k$  is the gain that depends on system design and relates to the turn rate of the UAV. Let  $T_{W_i, W_{i+1}}$  be the time taken by the UAV to traverse from waypoint  $W_i$  to waypoint  $W_{i+1}$ . This can be estimated by

$$T_{W_i, W_{i+1}} \approx \int dt, \text{ until } \|(x, y)^\top - W_{i+1}\| < \rho \quad (23)$$

**Table 1** UAV model and controller parameters

Parameter	Value	Parameter	Value
$\rho$	120 m	$v_a$	40 m/s
$v_w$	0, 9, 15 m/s	$\psi_0$	0
$\psi_w$	$\pi/4$	$G_i$	10 dB
$G_j$	10 dB	$G_u$	10 dB
$h_i, h_j$	20 cm	$h_u$	200 m
$X_u$	2.5 km	$Y_u$	-5 km
$X_{max}$	5 km	$Y_{max}$	5 km
$P_{t0}$	33 dB	$f$	5.8 GHz
$B$	1 MHz	$P_{rmin}$	-95 dB
$M$	8	$K$	10 dB
$R_b$	2 dB	$R_0$	1 Mbit/s
$E_{RX}$	50 nJ/s/bit	$E_{DA}$	5 nJ/s/bit
$E_{TX}$	50 nJ/s/bit	$N_0$	-110 dB
$l$	800 B	$l_{ctr}$	200 bit
$N$	200	$N^{\text{Iterations}}$	5000
$\alpha_1$	100	$\alpha_2$	$10^5$
$\alpha_3$	$10^{-3}$	$E_0$	1 J
<i>Simulations</i>	500	$N^{\text{CH}}$	5, 10, 20

where  $\rho$  is the minimum turn radius of the UAV. For data mule applications, we assume the UAV flies at a constant height and changes its heading depending the path and hence we assume the model of UAV to be a Dubins car model [39].

Assuming that the UAV needs to start from its original position ( $W_0$ ), visits all the waypoints  $W_i$  ( $i \in \{1, \dots, N^{\text{CH}}\}$ ), and return to its starting point, then the total time taken by the UAV to complete one round is

$$f_3 = T_{W_{N^{\text{CH}}}, W_0} + \sum_{i=0}^{N^{\text{CH}}-1} T_{W_i, W_{i+1}}. \quad (24)$$

For a given path with waypoints, the UAV has to follow the path under wind. There are several path following algorithm that can be used for the UAV to follow the path [40]. We use vector-field path following algorithm for the UAV to follow the path determined the PSO algorithm [41]. The model (22) is used in our simulations since it is a very simple model. More accurate results could be achieved by using a flight simulator including the aerodynamics and flight control of the actual UAV, at an additional computation cost.

## 4 Simulation results

### 4.1 Simulation setup

Monte-Carlo simulations are conducted for both LEACH-C and PSO schemes with different number of cluster head nodes (5, 10, and 20), and wind effects ( $v_w = 0$  and  $v_w > 0$ ). The UAV air speed is 40 m/s. The number of sensor nodes in the network is 200 at the beginning of each simulation scenario and other assumptions,

conditions are the same while simulating for LEACH-C and PSO algorithms. The nodes are randomly ( $\mathcal{N}(0, 1)$ ) generated in a region of  $25 \text{ km}^2$  area. Initially, all the nodes have the same energy  $E_0$ .

Each simulation lasts for a maximum of 500 sorties or until all of the nodes in the network run out of power from the battery. For each sortie, the PSO algorithm determines the CHs that need to be visited by the UAV majorly taking the current energy levels of the nodes into account. In the algorithm, the positions of the nodes in the network also affects the solution which needs to jointly minimize the energy consumption, erroneous bits, and flight time for the UAV. Since the nodes are not movable in this assumption, it could be said that the CH selection is basically based on current energy levels of the nodes, and the selected CHs for the current sortie can therefore be different from the previous sortie. After each sortie, the energy levels of the nodes are reduced depending on the amount of data communicated acting either as a CH or as a member node. In the PSO algorithm that is called at the beginning of each sortie, the number of iterations is applied with  $N^{\text{Iterations}} = 5000$ . Regarding to weighting constants set in these main simulations, they are selected with the priority orders as following: BER, Energy, and then travelling time of the UAV. It is further discussed in details how to select these constants in Section 4.3.

All other parameters related to UAV flight, data communication and simulation conditions are shown in Table 1. It is assumed that both sensor nodes and the UAV are equipped with directional antenna systems (i.e. phased array), and the beams of both the transmitter and receiver will point to each other during their communication thanks to the shared knowledge of their exact positions. This assumption is used in calculating the receiving signal strengths in equations (10) and (14). These estimations are then used to calculate SNR as well as the according transmission bit rate for data transmission in a specific case. Such small phased array antennas have been used in some UAV applications, for instance at [42]. The UAV is assumed to fly at a constant altitude of 200 m and ground speed of 40 m/s with a minimum turning radius of 120 m. The simulations illustrate all the terms in the fitness function, which include average energy consumption in the network, average BER, and travelling time for the UAV. Additional results such as the total of alive/dead node during simulation rounds, tracking of dead node's time, and the value of the fitness function returned from both LEACH-C and PSO schemes are also analyzed.

## 4.2 Comparisons of LEACH-C and PSO Algorithms without Wind

This Section will illustrate how the PSO scheme outperforms LEACH-C. For its simplicity, we can consider the case that BER is the highest priority concerned amongst the three constraints of energy, BER, and time. In practice, there is a relevance between BER and energy because BER would be improved when a node and its CH node is closer; or when a CH node and UAV is closer; and these situations always cause less energy consumption. Otherwise, a high BER also leads to a need for re-transmission, and hence more energy consumption. Again, this comparison between PSO and LEACH-C is conducted with the most expectation is to reduce the BER, and the results are referred in following Figure 1, 2, and 3. The performances for energy consumption and BER indicated that PSO achieves a better performance compared to LEACH-C under the same initial simulation condition and network topology. With the common trend from these figures, it shows that the higher number of CH nodes applied in the network the lower the energy consumption, BER, and therefore higher number of alive nodes remaining in the network. In addition, the gap in performances of the LEACH-C and PSO schemes will be more visible when increasing the number of CH nodes. The improved performance of PSO compared to LEACH-C could be seen from Figure 4 where the fitness values are almost kept constant with the PSO scheme at the beginning and then start to decrease after a certain number of rounds. However, with LEACH-C scheme, the fitness values seems unpredictable, such as they increase a little bit at the beginning, reduce at the middle, and then increase again even when there are few number of alive node in the network. This means that PSO has found a better selection of CH nodes where returned a more stable and lower cost in general. The plausible reason of why the PSO's fitness value is gradually decreasing and become very small at the right edge is that, at that moment many of the nodes are dead but the number of CHs is still unchanged; hence, the ratio of nodes that have direct communication with the UAV is increased. This makes the BER and the traveling time for the UAV decrease. However, this trend is difficult to predict in the case with LEACH-C because of the random selection of the CH nodes.

Further analysis is shown in Figure 5 and 6 where the positions of the nodes and tracking of their time-of-death are simultaneously depicted. The figures show that all the nodes in the network are dead after running nearly 300 times of data collection in the LEACH-C case, while there are still many alive nodes in the



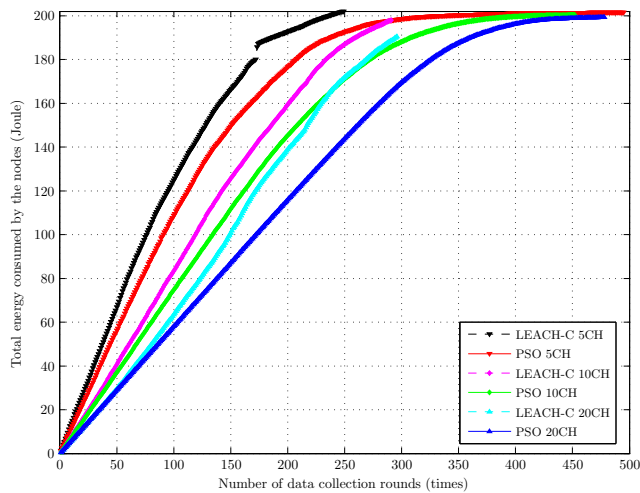


**Fig. 1** Total energy consumption by the nodes as a function of the number of data collection rounds for  $N^{CH} \in \{5, 10, 20\}$  and  $v_w = 0$ .

network with the PSO scheme even after running 500 rounds of simulation. The colors of the nodes are associated with the round or iteration when the nodes died due to energy drainage. In Figure 5, with LEACH-C, the nodes with the same colors are usually located in the same areas, and they are not as evenly distributed as the dead nodes in Figure 6 where the PSO is applied. The LEACH-C algorithm may attempt to select many CHs from one of these areas in the same round because they are close to each other and therefore can reduce the values of the fitness function. The difference between the dead nodes distribution in LEACH-C and PSO could be the answer to why the traveling time for the UAV with PSO is not better than with the LEACH-C scheme, as shown in Figure 7. These results show that the UAV requires even a little longer time to collect data each round with the PSO scheme, but the PSO scheme always provides a better overall fitness value compared to LEACH-C.

#### 4.3 Effect of Weighting Factors on Performance

This Section will illustrate more results only for PSO algorithm. This shows the differences in performances when energy, or time is set at the highest priority to the optimization process (as BER was considered in the results above).

As introduced in the fitness function (8), the weighting factors are  $\alpha_1$ ,  $\alpha_2$ , and  $\alpha_3$ , associated with the three sub functions  $f_1$ ,  $f_2$ , and  $f_3$ . These sub functions are representative for the energy consumption, bit-error-rate, and UAV travelling time, respectively. We can define the three cases in which energy consumption, BER, or time is the most prioritized in the optimization. For

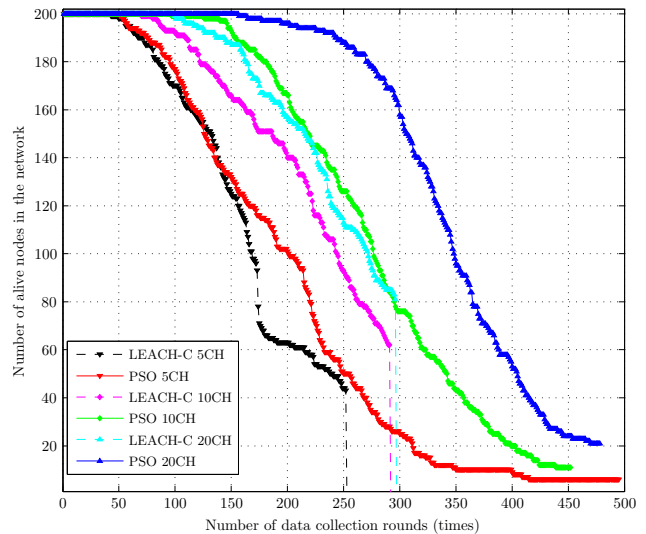


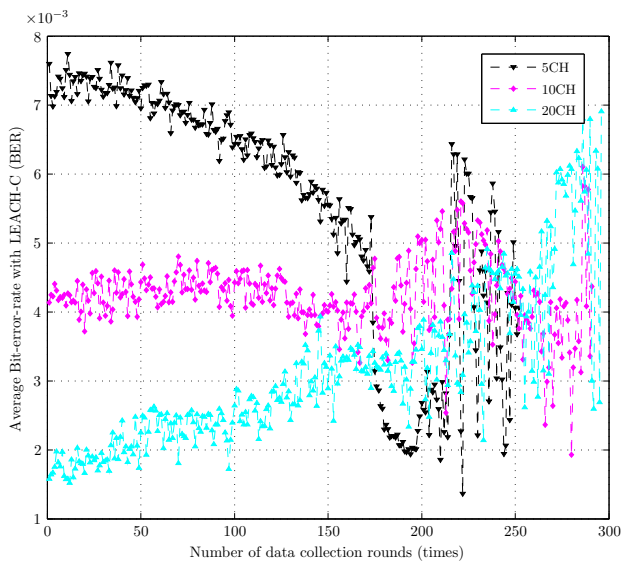
**Fig. 2** The number of nodes alive in the network as a function of the number of data collection rounds for  $N^{CH} \in \{5, 10, 20\}$  and  $v_w = 0$ .

**Table 2** Different Weight Factors in Fitness Function

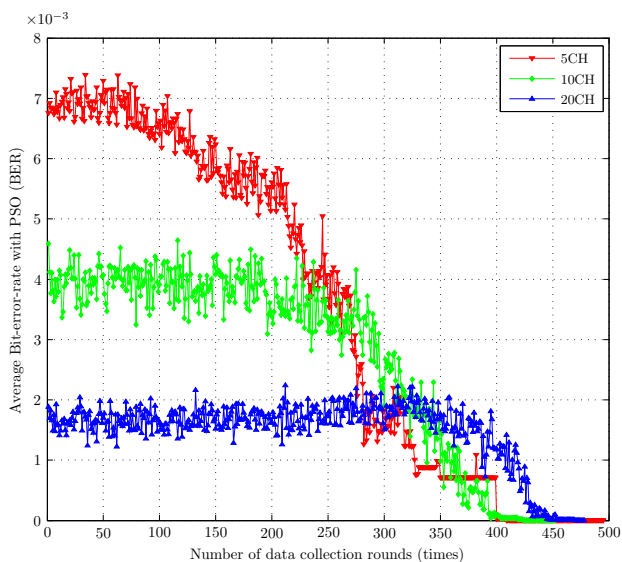
Three scenarios	$\alpha_1$	$\alpha_2$	$\alpha_3$
Case 1 (Energy)	$10^5$	$10^2$	$10^{-3}$
Case 2 (BER)	$10^2$	$10^5$	$10^{-3}$
Case 3 (Time)	$10^{-1}$	$10^2$	1

the case  $i$ , the according weight factor  $\alpha_i$  would be selected with the condition that  $\alpha_i f_i$  is significantly larger than  $\alpha_j f_j$ ,  $j \neq i$ . Table 2 provide example values for  $\alpha_i$  in those cases ( $i = 1, 2, 3$ ).

The changes of weight factors would directly affect the fitness function. The most visible factor that could affect the general network performance is the energy usage. The results in Figure 8 are based on the simulation conditions as in other cases (with parameters in Table 1) except (i) the weight factors which are selected from the three cases in Table 2 and (ii) only the case of 5 waypoints is simulated and plotted. From the variations in Figure 8, the number of dead nodes in the first two cases (cases 1, 2) are quite similar and much lower than the one in the third case. It means the nextwork lifetime is extended when energy or BER is the most concern for PSO algorithm. The travelling time periods for the UAV are not emphasized here as it is not as highly concerned as energy and BER in this paper. However, the time in the third case would theoretically be much lower than that in the other two cases. When travelling time is mostly concerned, the PSO scheme would try to find the set of CHs that the UAV need the least time to fly over them. In this case, there would be a high possibility of suffering high energy for message exchange and data communication, especially amongst the nodes as its large propagation path



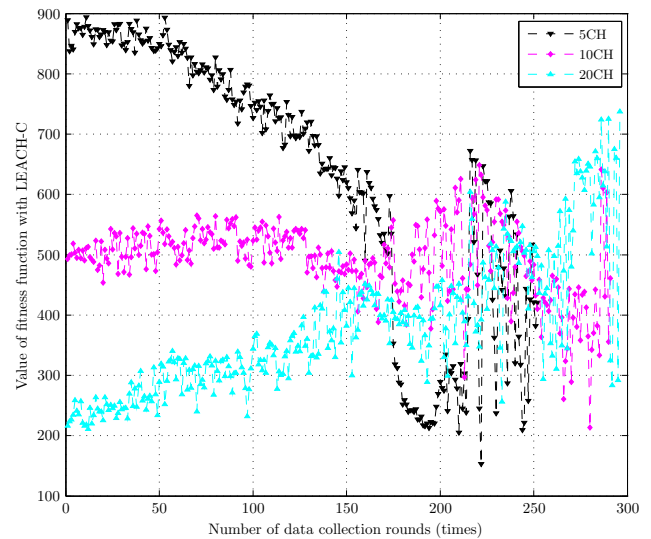
(a) with LEACH-C



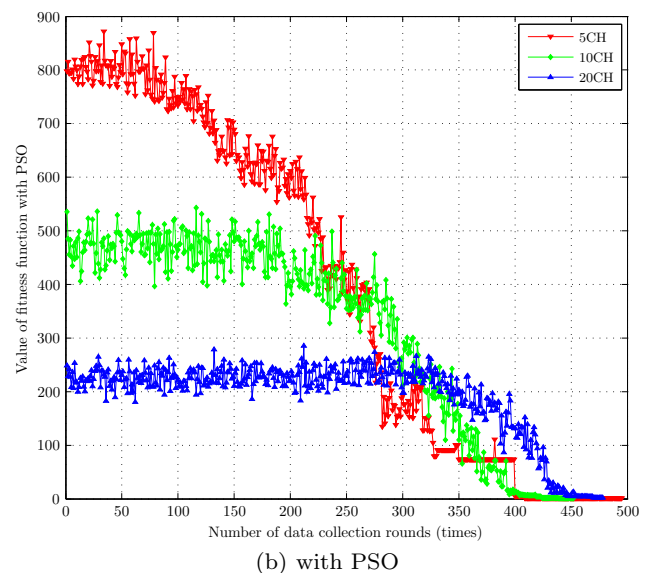
(b) with PSO

**Fig. 3** Bit-error-rate as a function of number of data collection rounds for  $N^{\text{CH}} \in \{5, 10, 20\}$  and  $v_w = 0$ .

loss. As mentioned above, there is a close relation between BER and energy, as a result, the performance in term of the dead node numbers is quite similar in these two cases. Further analysis in simulations show that the priority orders in cost function for the first case are energy, BER, and travelling time; for the second case are energy, BER, and travelling time. The travelling time of the UAV is just a minor cost in the main cost function of PSO for the first two case; hence, it does not affect to the overall performance. It would be clearer to see this effect of weighting constants changes on how the UAV was flying over the waypoints for data acquisition. For the simplicity of graph, one example data is plotted in



(a) with LEACH-C



(b) with PSO

**Fig. 4** Fitness value  $f$  for  $N^{\text{CH}} \in \{5, 10, 20\}$  and  $v_w = 0$ .

Fig 9 when there was 50 alive nodes in the network and all other parameters are same as the ones used for plotting Fig 8. From these discussed results on both Figures 8 and 9, this Section provides insight explanations on how to select the most reasonable weight factors base on the most expectation for the network, as well as how this selection affected on the network performances.

#### 4.4 Evaluation of PSO under Wind Effect

In Section 4.2, the PSO scheme outperforms LEACH-C in terms of energy consumption, BER, and total fitness value under the no-wind condition. This section will therefore only show the impact of the wind using the PSO scheme. Other conditions and assumptions are the

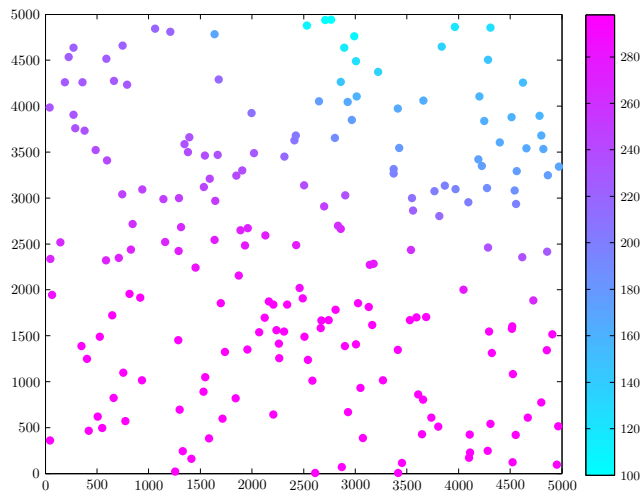


**Fig. 5** Node distribution for  $N^{\text{CH}} = 20$  and  $v_w = 0$  using LEACH-C. The color represents the iteration number when each node ran out of energy. After approximately 300 rounds, all nodes are dead.

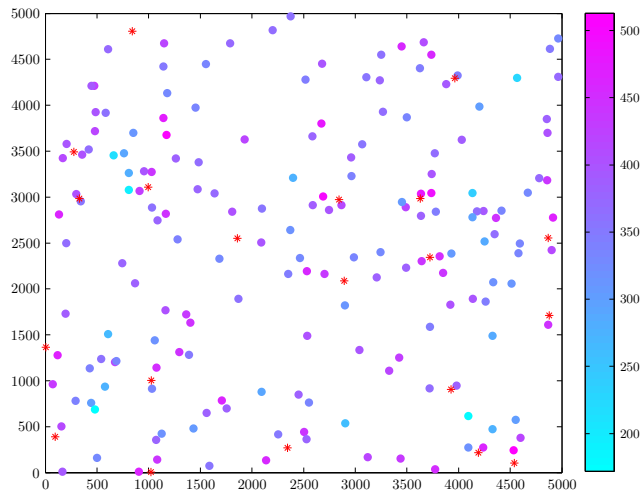
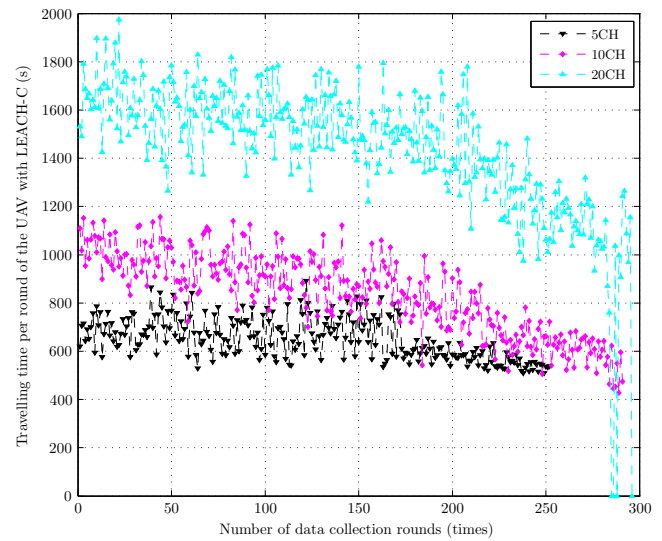
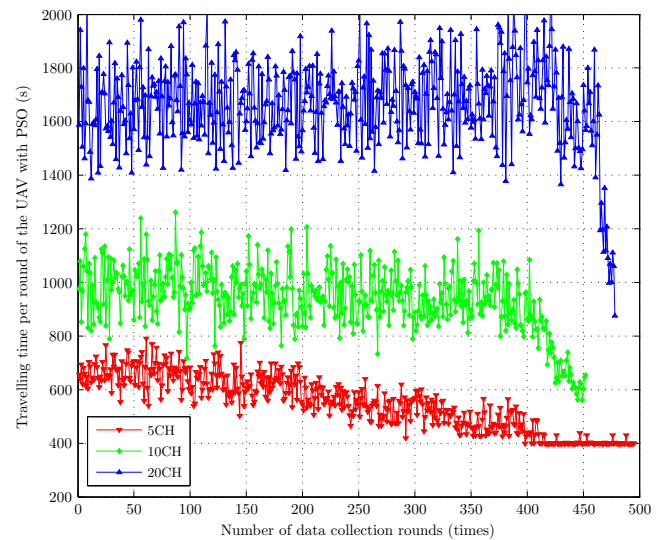


**Fig. 6** Node distribution for  $N^{\text{CH}} = 20$  and  $v_w = 0$  using PSO. The color represents the iteration number when each node ran out of energy. After 520 rounds, there are still nodes alive (denoted by a red star).

same as implemented in Section 4.2. For simplicity we assume that the wind is steady and uniform; hence, the wind speed and direction is the same for all the points of the flight. With the wind effect, as shown in (22), the ground speed of the UAV could be decreased or increased depending on the relative direction of the UAV and the wind at each moment. When the UAV is flying against the wind, its ground speed is decreased and needs more time to visit the waypoints (CHs). When the wind is from behind, the UAV speed is increased. In these simulations, total energy consumption and BER are prioritized in the fitness function (8), and these factors are not much affected by the windy environment. This result could be seen by the similarities of the pairs



(a) with LEACH-C



(b) with PSO

**Fig. 7** Travelling time for the UAV to finish one round of data collection for  $N^{\text{CH}} \in \{5, 10, 20\}$  and  $v_w = 0$ .

of lines representing the cases of wind at 0 m/s and 15 m/s in Figure 10, Figure 11, and Figure 12. However, the effect of wind on the traveling time for the UAV is more visible as shown in Figure 13. In the windier environment, the the UAV needs more time in order to visit all the waypoints. The results in Figure 14 also agree with this trend, that the optimal fitness value returned from PSO scheme in a windy condition is slightly larger than that with no wind effect condition.

In order to show the effect of wind on the UAV flight, Figure 15 shows in details how the UAV was flying over the selected waypoints under the constraint that BER and energy were the most concerns. The UAV route in the windless case is reused from the result of case 2 that was shown in Figure 9, so there would be

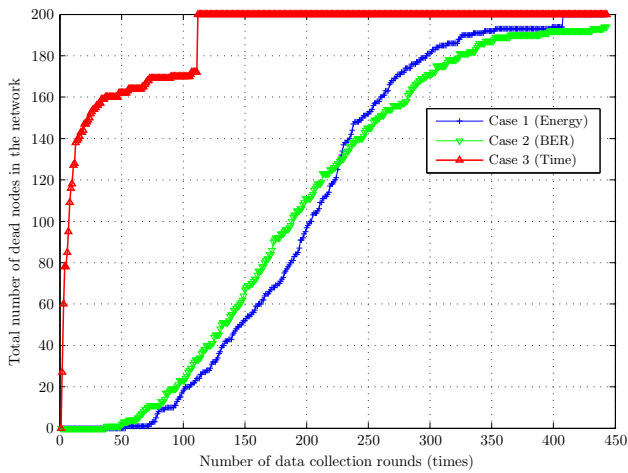


**Fig. 8** The number of dead nodes in the network when energy, BER, or time is in turn the most priority of PSO (with 5 CHs).

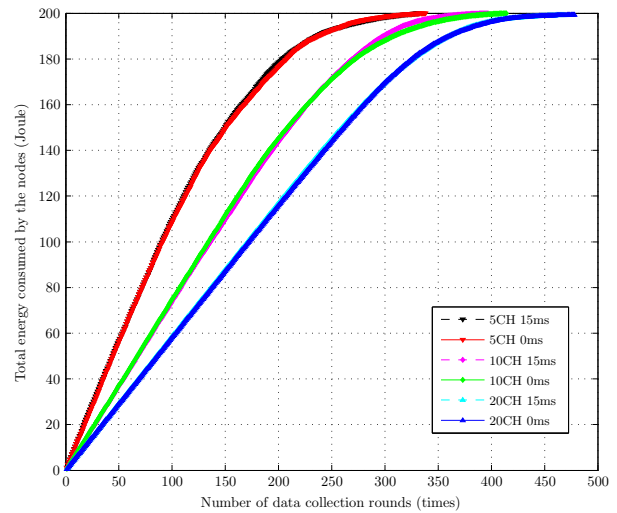


**Fig. 10** Comparison of energy consumption in PSO scheme with  $N^{\text{CH}} \in \{5, 10, 20\}$  and  $v_w \in \{0, 15\}$ m/s.

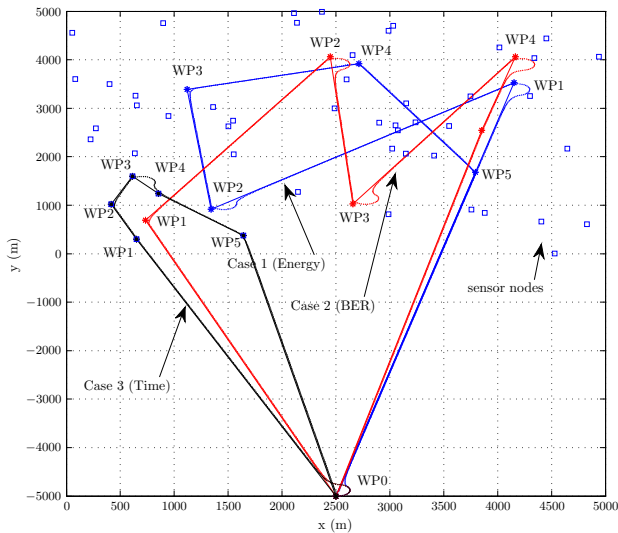


**Fig. 9** The UAV paths in the cases energy, BER, or time is in turn the most priority of PSO (with 5 CHs and 50 sensor nodes).

5 waypoints (CHs) and 50 alive sensor nodes; other assumptions are similar as being used for plotting Figure 9. Also, the same algorithm was applied for the UAV movements in both the cases of windless and windy. The results from this Figure 15 show that these flight routes of the UAV might be not the shortest ones but they would minimize BER and energy consumption as the travelling time was not the highest concern in this case. Due to the effect of the wind at a certain wind direction ( $\pi/4$  this case), there is some difference in the flight path when the UAV changes its direction at some sharp angles. In Figure 15, the stars represent for the waypoints and the squares are for the sensor nodes in the network. The red and green dots are for the movements of the UAV in windless and windy (at a speed

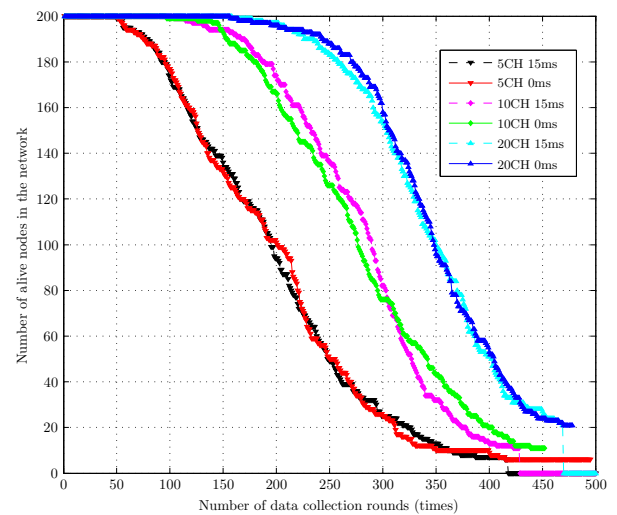


**Fig. 11** Comparison of alive nodes in PSO scheme with  $N^{\text{CH}} \in \{5, 10, 20\}$  and  $v_w \in \{0, 15\}$ m/s.

of 15m/s) conditions, respectively. In Figure 15, we can also see that the UAV is far away from the location of the nodes. This assumption is based on a practical situation where these nodes are located on a remote area that is quite separated from initial location of the UAV.

#### 4.5 Discussions

As in any multiobjective optimization problem, the relative weighting of the objectives is difficult. Some rule-of-thumb exists in the literature, such as scaling each objective by the optimal value of this objective when known. Another recommendation is to scale the initial guess, such that the cost of each individual objective is 1 at start-up. These rules are not always easily applicable, and for similar multiobjective covering salesperson

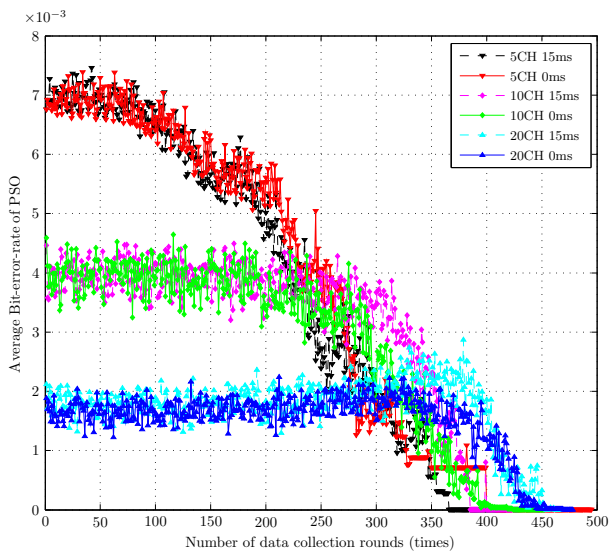


**Fig. 12** Comparison of BER in PSO scheme with  $N^{CH} \in \{5, 10, 20\}$  and  $v_w \in \{0, 15\}$ m/s.

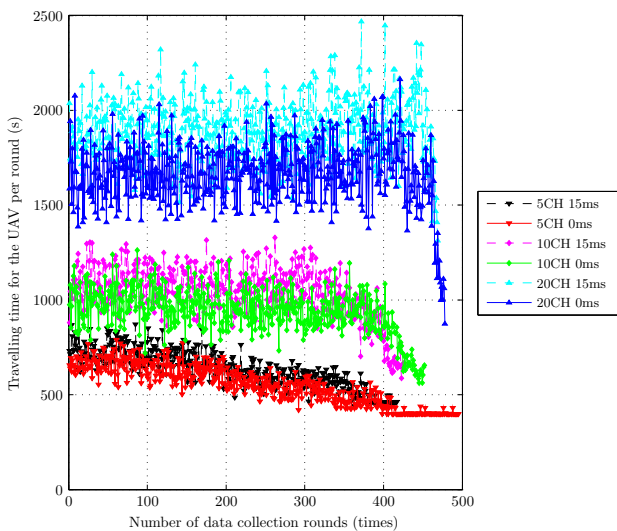


**Fig. 13** Comparison of travelling time of the UAV in PSO scheme with  $N^{CH} \in \{5, 10, 20\}$  and  $v_w \in \{0, 15\}$ m/s.

problems we encourage the reader to make the relative weighting based on simulation studies and practical judgement of the resulting performance. For instance, one can consider what is truly the benefit of reducing the travel time in our path planning problem. The main reason to reduce the traveling time would be related to the operation cost in the UAV operation or the endurance of the UAV. One of more human operators may need to supervise the operation. However, when the purpose is to collect as much information as possible in a continuous operation, it is apparent that reducing the time of each individual run can be less emphasized. A second argument for reducing the travel time, is the want to reduce the latency from the obser-

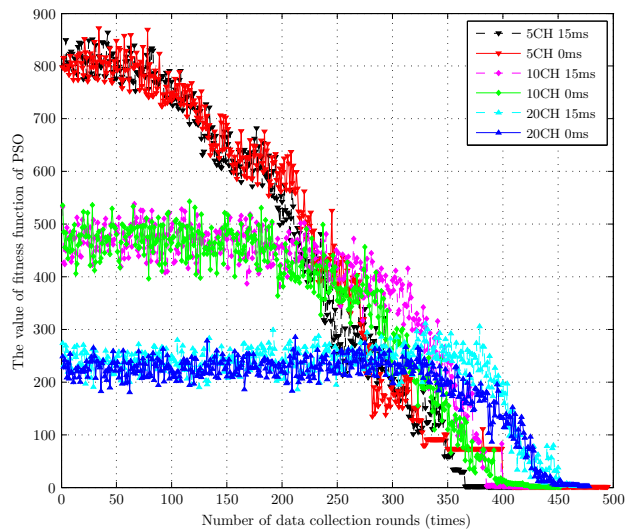


**Fig. 14** Comparison of Fitness values in PSO scheme with  $N^{CH} \in \{5, 10, 20\}$  and  $v_w \in \{0, 15\}$ m/s.

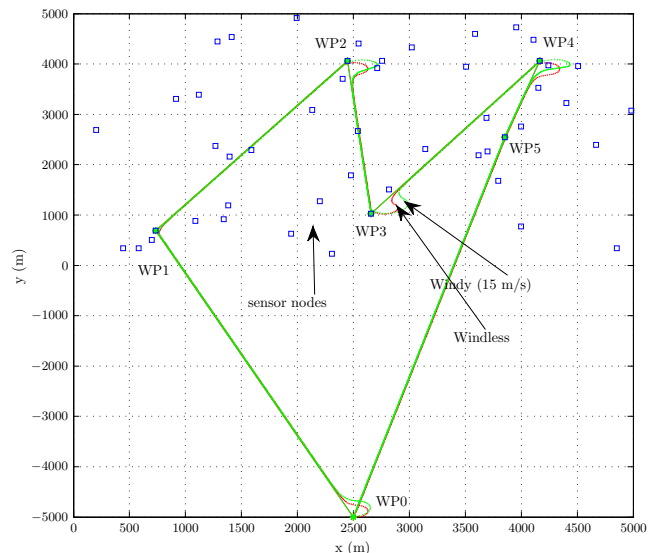


**Fig. 15** How UAV flies over the waypoints in windless and windy conditions when BER is the most constraint (with 5 CHs and 50 sensor nodes).

vation until the data is received by the user requesting the sensor information. Obviously this is depending on the process to be observed by the sensors, but due to the latency already experienced while data is stored on the sensor nodes, we believe that decreasing the travel time of each individual run will have limited impact on the overall delay.

For a practical implementation of the proposed algorithm the following should be considered. The autopilot will need to be equipped with a Global Navigation Satellite System (GNSS) receiver, a computer, radio system, and a directional antenna. Most UAVs for outdoor flying have a GNSS receiver as part of their

navigation system, and will be used to update the information about the UAV's own position. The computer will do the datalogging, and control the communication. Regarding to waypoints optimization, the model for estimating the UAV travelling time in this paper is simple and it would be straightforward to replace with a sophisticated flight simulators at the expense of additional computation time. For the antennas on both the sensor nodes and the UAV, they could be attached with a standard dipole or patch antenna, or a patch antenna on each node and a phased array antenna on the UAV. The assumption of using directional antennas in this paper is to provide the beam-forming function, capability of extending the communication distance, as well as saving energy or maximizing the network lifetime. In the case of using dipole antennas on the nodes and the UAV, the energy on the node would be running out much quicker; hence, the network lifetime would significantly reduced. The location of the nodes need to be known by the path planning algorithm, but since we consider static nodes it is reasonable to assume that this information can be uploaded to the UAV before the mission starts. As already pointed out, we also assume that sensor nodes are equipped with a suitable radio and antenna, in addition to a battery, a computer and one or more sensors appropriate for the process to be observed.

## 5 Conclusions

In this article, we have evaluated the performance of two algorithms for optimal selection of the cluster heads (wide area WSNs) which are transferred to the UAV as the waypoints for its data acquisition. In our objective function, the energy consumed by the network, communication quality, and traveling time for the UAV are optimized with the PSO algorithm. Any or all of them could be the dominant factor to the optimization algorithm, and the effect of these variations have been studied. In the main simulations for comparison with LEACH-C, we have given the highest priority to the average BER, and lower ones for energy consumption and traveling time of the UAV. PSO has shown that it outperforms the LEACH-C scheme when applied to optimization for wide area sensor networks and UAV data acquisition. Our simulations also show that the life time of the network can be significantly extended using the optimization scheme. Furthermore, performance evaluations of the scheme have also been further developed and examined under the effect of the wind. In the case we continue to keep priorities for BER and energy consumption, these criteria are not significantly affected

by the wind. The traveling time, however, is affected by the wind speed.

**Acknowledgements** The work is supported by the Research Council of Norway and Statoil through the Center for Autonomous Marine Operations and Systems (AMOS), and the Strategic University Program on Control, Information, and Communication Systems for Environmental and Safety Critical Systems. This work was carried out during the tenure of an ERCIM Alain Bensoussan Fellowship Program. This Programme is supported by the Marie Curie Co-funding of Regional, National and International Programs (COFUND) of the European Commission. This work is partially supported by the Fundação para Ciência e Tecnologia under project PTDC/EEA-ELC/122203/2010.

## References

1. K. Purvis, K. Åström, and M. Khammash, "Estimation and optimal configurations for localization using cooperative UAVs," *IEEE Trans. on Control System Technology*, vol. 16, pp. 947–958, 2008.
2. E. W. Frew and T. X. Brown, "Networking issues for small unmanned aircraft systems," *J. of Int. and Robotic Sys.*, vol. 54, pp. 21–37, 2008.
3. J. J. Ruz, O. Arevalo, G. Pajares, and J. M. De la Cruz, *UAV trajectory planning for static and dynamic environments*. InTech, 2009, ch. 27, pp. 581–600.
4. E. F. Flushing, L. Gambardella, and G. Di Caro, "Search and rescue using mixed swarms of heterogeneous agents: Modeling, simulation, and planning," IDSIA/USI-SUPSI, Tech. Rep., 2012.
5. T. Brown, B. Argrow, C. Dixon, S. Doshi, R. Thekkekkunnel, and D. Henkel, "Ad hoc UAV-ground network (AUGNet)," in *Proc. of the AIAA 3rd Unmanned Unlimited Technical Conference, Workshop and Exhibit*, 2004.
6. D. T. Ho, E. I. Grøtli, S. Shimamoto, and T. A. Johansen, "Optimal relay path selection and cooperative communication protocol for a swarm of UAVs," in *Proc. of the 3rd International Workshop on Wireless Networking & Control for Unmanned Autonomous Vehicles: Architectures, Protocols and Applications*, 2012, pp. 1585–1590.
7. P. B. Sujit, D. E. Lucani, and J. B. Sousa, "Bridging cooperative sensing and route planning of autonomous vehicles," *IEEE Journal on Selected Areas in Communications*, vol. 30, pp. 912–922, 2012.
8. J. Isaacs, S. Venkateswaran, J. Hespanha, U. Madhoo, J. Burman, and T. Pham, "Multiple event localization in a sparse acoustic sensor network using UAVs as data mules," in *Proc. of the 3rd International Workshop on Wireless Networking & Control for Unmanned Autonomous Vehicles: Architectures, Protocols and Applications*, 2012, pp. 1562–1567.
9. F. Wang and J. Liu, "Networked wireless sensor data collection: Issues, challenges, and approaches," *IEEE Communications Surveys & Tutorials*, vol. 13, pp. 673–687, 2011.
10. L. He, J. Tao, J. Pan, and P. Xu, "Adaptive mobility-assisted data collection in wireless sensor networks," in *Proc. of the International Conference on Wireless Communications and Signal Processing*, 2011, pp. 1–6.
11. W. Liang, J. Luo, and X. Xu, "Prolonging network lifetime via a controlled mobile sink in wireless sensor networks," in *Proc. of the 2010 IEEE Global Telecommunication Conference (GLOBECOM)*, 2010, pp. 1–6.

12. L. Tong, Q. Zhao, and S. Adireddy, "Sensor networks with mobile agents," in *Proc. of the 2003 IEEE Military Communications Conference*, vol. 1, 2003, pp. 688–693.
13. D. T. Ho and S. Shimamoto, "Highly reliable communication protocol for WSN-UAV system employing TDMA and PFS scheme," in *Proc. of the 2nd International Workshop on Wireless Networking & Control for Unmanned Autonomous Vehicles: Architectures, Protocols and Applications*, 2011, pp. 1320–1324.
14. D. T. Ho, E. I. Grøtli, and T. A. Johansen, "Heuristic algorithm and cooperative relay for energy efficient data collection with a UAV and WSN," in *Proc. of the IEEE International Conference on Computing, Management & Telecommunications*, 2013, pp. 346–351.
15. E. I. Grøtli and T. A. Johansen, "Path planning for UAVs under communication constraints using SPLAT! and MILP," *Journal of Intelligent and Robotic Systems*, vol. 65, no. 1-4, pp. 265–282, 2012.
16. —, "Path- and data transmission planning for cooperating UAVs in delay tolerant network," in *Proc. of the 3rd International Workshop on Wireless Networking and Control for Unmanned Autonomous Vehicles: Architectures, Protocols and Applications*, 2012, pp. 1568–1573.
17. A. Grancharova, E. I. Grøtli, and T. A. Johansen, "Distributed MPC-based path planning for UAVs under radio communication path loss constraints," in *Proc. of the IFAC Conference on Embedded Systems, Computational Intelligence and Telematics in Control*, 2012, pp. 254–259.
18. K. Zhang, E. G. Collins Jr, and A. Barbu, "An efficient stochastic clustering auction for heterogeneous robotic collaborative teams," *Journal of Intelligent & Robotic Systems*, vol. 72, no. 3-4, pp. 541–558, 2013.
19. K. Zhang, E. G. Collins Jr, and D. Shi, "Centralized and distributed task allocation in multi-robot teams via a stochastic clustering auction," *ACM Transactions on Autonomous and Adaptive Systems (TAAS)*, vol. 7, no. 2, p. 21, 2012.
20. J. Tsitsiklis, "Efficient algorithm for globally optimal trajectories," *IEEE Trans. Autom. Contr.*, vol. 40, no. 9, pp. 1528–1538, 1995.
21. Q. Zhao and L. Tong, "Quality of service specific information retrieval for densely deployed sensor network," in *Proc. of the 2003 IEEE Military Communications Conference*, vol. 1, 2003, pp. 591–596.
22. M. Salari and Z. Najj-Azimi, "An integer programming-based local search for the covering salesman problem," *J. of Computer & Operations Research*, pp. 2594–2602, 2012.
23. S. Shi, L. X., and X. Gu, "An energy-efficiency optimized LEACH-C for wireless sensor networks," in *Proc. of the International ICST Conference on Communication and Networking in China (CHINACOM)*, 2012, pp. 487–492.
24. W. Heinzelman, A. Chandrakasan, and H. Balakrishnan, "An application-specific protocol architecture for wireless microsensor networks," *IEEE Trans. on Wireless Communications*, vol. 1, pp. 660–670, 2002.
25. A. Ghaffarkhah and Y. Mostofi, "Communication-aware motion planning in mobile networks," *IEEE Transaction on Automatic Control*, vol. 56, no. 10, pp. 2478–2485, 10 2011.
26. "SPLAT! - an RF Signal Propagation, Loss, And Terrain analysis tool," Accessed: November 2014. [Online]. Available: <http://www.qsl.net/kd2bd/splat.html>
27. N. M. A. Latiff, C. C. Tsimenidis, and B. S. Sharif, "Energy-aware clustering for wireless sensor networks using particle swarm optimization," in *Proc. of the IEEE International Symposium on Personal, Indoor and Mobile Radio Communications*, 2007, pp. 1–5.
28. B. Singh and D. Lobiya, "A novel energy-aware cluster head selection based on particle swarm optimization for wireless sensor networks," *Journal of Human-centric Computing and Information Sciences*, vol. 2, pp. 1–18, 2012.
29. J. Kennedy and R. Eberhart, "Particle swarm optimization," in *Proceedings of IEEE International Conference on Neural Networks*, vol. 4, 1995, pp. 1942–1948.
30. K. E. Parsopoulos and M. N. Vrahatis, "Recent approaches to global optimization problems through particle swarm optimization," *Natural computing*, vol. 1, no. 2-3, pp. 235–306, 2002.
31. I. C. Trelea, "The particle swarm optimization algorithm: convergence analysis and parameter selection," *Information Processing Letters*, vol. 85, pp. 317–325, 2003.
32. Y. Shi and R. C. Eberhart, "Parameter selection in particle swarm optimization," in *Proc. of the International Conference on Evolutionary Programming*, 1998, pp. 591–600.
33. M. E. H. Pedersen and A. J. Chipperfield, "Simplifying particle swarm optimization," *Applied Soft Computing*, vol. 10, pp. 618–628, 2010.
34. H. W. Kuhn, "The Hungarian method for the assignment problem," *Naval Research Logistics Quarterly*, vol. 2, pp. 83–97, 1955.
35. A. Goldsmith, *Wireless Communications*. Cambridge University Press, 2005.
36. D. T. Ho, J. Park, S. Shimamoto, and J. Kitaori, "Performance evaluation of multi hop relay network for oceanic air traffic control communication," *IEICE Transactions on Communications*, vol. E94-B, no. 1, pp. 86–96, 2011.
37. D. T. Ho, E. Grøtli, P. Sujit, T. Johansen, and J. Borges Sousa, "Cluster-based communication topology selection and UAV path planning in wireless sensor networks," in *Proc. of International Conference on Unmanned Aircraft Systems (ICUAS)*, 2013, pp. 59–68.
38. K. Savla, E. Frazzoli, and F. Bullo, "Traveling salesperson problems for the Dubins vehicle," *IEEE Transaction on Automatic Control*, vol. 53, pp. 1378–1391, 2008.
39. L. E. Dubins, "On curves of minimal length with a constraint on average curvature, and with prescribed initial and terminal positions and tangents," *American Journal of mathematics*, pp. 497–516, 1957.
40. P. Sujit, S. Saripalli, and J. Sousa, "Unmanned aerial vehicle path following: A survey and analysis of algorithms for fixed-wing unmanned aerial vehicles," *Control Systems, IEEE*, vol. 34, no. 1, pp. 42–59, 2014.
41. D. R. Nelson, D. B. Barber, T. W. McLain, and R. W. Beard, "Vector field path following for miniature air vehicles," *IEEE Transactions on Robotics*, vol. 23, no. 3, pp. 519–529, 2007.
42. V. E. Hovstein, A. Sægrov, and T. A. Johansen, "Experiences with coastal and maritime UAS BLOS operation with phased-array payload data link," in *Proc. of International Conference on Unmanned Aircraft Systems (ICUAS)*, May 2014.